minerals

MDPI

Article

Evaluating the Potential of Gold Compositional Studies to Contribute to the Early Stages of Exploration Programs

Robert Chapman [1,*], Taija Torvela [1], Aiden Lavelle [2], Kevin Dalton [3], Gregor Donaghy [4], Shane Webb [5], Lucia Savastano [6], Kieran Armstrong [7] and Richard Walshaw [1]

[1] Ores and Mineralization Group, School of Sustainability, Earth and Environment, The University of Leeds, Leeds LS2 9JT, UK; t.m.torvela@leeds.ac.uk (T.T.); r.d.walshaw@leeds.ac.uk (R.W.)
[2] Green Glen Minerals Limited, The Threshing Barn, Manor Barns, Coates Lane, High Wycombe HP13 5UX, Buckinghamshire, UK; aiden@greenglenminerals.com
[3] Independent Researcher, 28 Garavogue Villas, Abbeyquarter, F91YR7R Sligo, Ireland
[4] Independent Researcher, Wester Balrobbie, Killicrankie, Perthshire PH16 5LG, Scotland, UK
[5] Département de Géologie et Génie Géologique, Université Laval, Quebec, QC G1V 0A6, Canada; shane.webb.1@ulaval.ca
[6] Tescan, Libušina Třída 21, 623 00 Brno, Czech Republic; lucia.savastano@tescan.com
[7] Northern Star Resources Limited, Level 4, 500 Hay Street, Subiaco, WA 6008, Australia
* Correspondence: r.j.chapman@leeds.ac.uk

Abstract

The outcomes of a standard geochemical, geophysical and petrographical approach to exploration at Lead Trial, a small prospect in central Scotland, have been compared to the interpretation of a parallel gold compositional study describing 703 gold particles from local in situ and alluvial occurrences. Standard exploration approaches identified a 4.5 km^2 zone hosting an array of numerous auriferous (to 17 g/t Au), vuggy, brecciated quartz-galena ± sphalerite veins culminating in the identification of a drill target. The gold study identified three gold compositional types: two 23–32 wt.% Ag alloys with a Zn-Pb-Cu mineral inclusion assemblage differentiated by sphalerite abundance, and a 5–16 wt.% Ag alloy with a Mo-Bi-Pb-Cu-Fe inclusion signature, yet to be correlated with either float or outcrop. Spatial distribution of the gold types indicates lateral variation and probably vertical variation within a single magmatic hydrothermal system. Integration of gold particle studies with early stages of exploration offers rapid insights into the nature and distribution of mineralization when very limited information is available and is mutually supportive of standard exploration approaches.

Keywords: alluvial gold; exploration; gold compositional studies

Check for updates

Academic Editor: Liqiang Yang

Received: 9 May 2026
Revised: 12 June 2026
Accepted: 17 June 2026
Published: 21 June 2026

1. Introduction

Identification of new gold targets and their subsequent characterization is often challenging because of varying degrees of surface cover [1]. In regions of poor exposure, known in situ gold occurrences may not account for the distribution of alluvial gold revealed either by sediment sampling programs [2], or in some cases economically viable placer mining operations [3]. In these situations, standard exploration targeting involves the application of an array of geochemical and geophysical approaches to infer the presence of this concealed mineralization and ultimately define a drill target. In a few cases, information has been gleaned by adopting gold compositional studies that have increased understanding of the local and regional gold mineralization, but relatively few studies have advocated the adoption of the approach early in exploration programs [4–6].

Gold compositional studies are finding increasing application worldwide as they provide information on the hypogene setting of source mineralization. Various studies have sought to identify the type of mineralization that has generated notable placer deposits, e.g., in Russia [7–9], Chile [10], Cameroon [11], Nigeria [12], Pakistan [13] and the Philippines [14], or to differentiate between different source types that have contributed to a single placer, e.g., in Russia [15,16]. Cameroon [17], Finland [18] and Spain [19]. Examples where signatures of alluvial gold do not fully correspond with those of known in situ local occurrences are of particular relevance to the present study. Notable examples include the identification of distinct gold subpopulations within the Anabar and Bolshaya Kuonamka river basins in Siberia, where gold from a palaeoplacer system exists alongside locally sourced in situ mineralization [20]. Placer gold from the Vagran placer cluster in the Northern Ural Mountains exhibited two main compositional types, one of which suggested the presence of undiscovered Carlin-type mineralization [21]. Similarly, in Yukon, Canada, alloy compositions of gold from the world-class Eldorado Creek placer are inconsistent with the microchemical signatures of gold particles from the historic Lone Star and Violet mine localities within the same valley catchment [22]. In such cases, characterization of gold from the in situ sources and their local alluvial expressions is valuable in both predicting the presence of further gold occurrences and in some cases indicating their likely economic importance [3].

Although in many cases information from the gold particles is the only route to gain further understanding of local or regional metallogeny, the approach remains an underutilized technique [4]. Nevertheless, its value to early-stage exploration and to defining the nature of concealed mineralization has been advocated [23] and summarized in two recent review papers [4,24]. In addition, synthesis of results from gold microchemistry with those from other exploration approaches such as stream sediment geochemistry [25] and regional structural analysis [26] can further constrain the location of undiscovered mineralization. In this contribution, we provide a case study of an early-stage exploration project located in central Scotland in which typical exploration approaches have progressed alongside gold compositional studies. This has provided the opportunity to both evaluate the contribution of the gold compositional work in this specific case and to identify generic outcomes of wider relevance.

Historical records of gold mineralization in central Scotland [27] indicated widespread occurrence within the Grampian Terrane. Regional stream sediment surveys and commercial prospecting in the 1980s identified gold-bearing veins at Calliachar Burn [28], Tombuie [29] and at Cononish where current operations target an outcome of 2000 oz per month [30]. Further exploration by Green Glen Minerals (previously Erris Gold Resources) between 2017 and 2020 identified gold-bearing lead–zinc mineralization at the Lead Trial prospect, near the southern shore of Loch Tay (Figure 1A), and joint work with the University of Leeds revealed polymetallic in situ veining in Glen Almond [31]. In addition to gold, of particular relevance to this paper is the historic small-scale Tomnadashan copper mine, which is hosted in a Silurian porphyry intrusion [32] (Figure 1A). The sulphide mineralization at Tomnadashan, which also hosts gold, is interpreted to be related to magmatic-hydrothermal activity and has been dated at c. 420 Ma [33].

The Lead Trial occurrence is an outcropping vein named after initial excavations to recover galena in the late 1800s [27]. Modern exploration was initiated by Green Ore in 2017, which entered into an Option Agreement with Erris Gold Resources in 2019, which was subsequently renamed Green Glen Minerals in 2021. This study focuses on the recent commercial exploration at Lead Trial and its environs together with a gold compositional study of both lode and alluvial material.

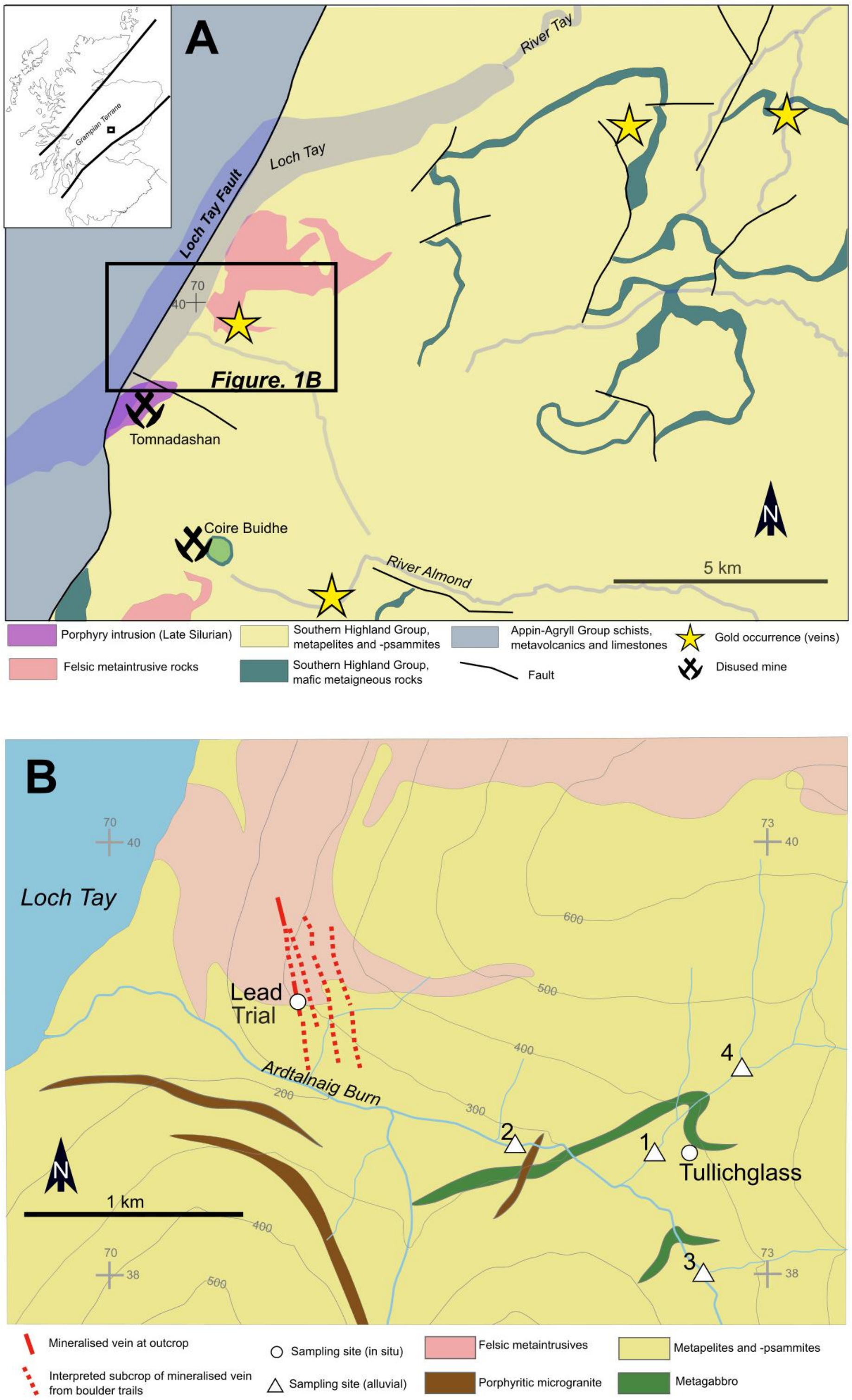

Figure 1. (**A**): Regional setting of study area. (**B**): Regional geology.

2. Deposit Description

2.1. Geographical Setting

The term 'Lead Trial' is used to denote a single, up to 1 m thick vein striking roughly NNW-SSE situated at the northern extremity of the Ardtalnaig Burn valley at an elevation of around 100 m above the valley floor (Figure 1B). The historical activities at Lead Trial generated spoil tips adjacent to the vein from which both mineralized samples and particulate gold were recovered during the present project. Lead Trial is one of several subparallel mineralized veins within a vein array that extends over 3 km along strike on the north side of the Ardtalnaig Burn valley (henceforward the Lead Trial Vein Array: LTVA). The Tullichglass locality is situated near the southern extremity of the LTVA. The mineralized float boulder sampled during the present project is at an elevation of around 50 m above Ardtalnaig Burn.

Ardtalnaig Burn flows roughly E-W, discharging directly into Loch Tay (Figure 1B). Exposure is very poor along the valley sides and non-existent at elevations below the Lead Trial outcrop owing to a blanket of unconsolidated glacial debris. The LTVA vein system does not appear to be present on the south side of the valley, although some thinner barren veining has been observed approximately along strike from the mineralised vein system. The Ardtalnaig Burn lies within a hanging valley, and the river gradient over the last kilometer of its length is very steep. Whilst bedrock is sometimes exposed in the stream bed at waterfalls, there are stretches that are choked with boulders weighing up to several tonnes.

2.2. Regional Geology

Recent studies of regional geology and metallogeny [28,29,34] and regional gold compositional studies [2] provide the regional context for the current study. In the LTVA, the dominant lithology is the Late Neoproterozoic to Cambrian Pitlochry schist formation of the Southern Highland Group, which comprises undifferentiated pelitic-psammitic rocks that form the overturned limb of the Tay Nappe [32] (Figure 1A). This sequence hosts both amphibolites and late Silurian and Devonian felsic and intermediate to felsic metaigneous rocks, chiefly as sub-parallel layers within the schist. The study area lies immediately East of the North-Northeast-trending Loch Tay fault, which is one of six major crustal faults within the Scottish Dalradian.

2.3. Deposit Geology

The account of the deposit geology presented in this section is based on information from exploration activity prior to 2017.

The lead-bearing veins at Ardtalnaig were first reported in a summary of mineral occurrences on the estate of the Marquis of Breadalbane in 1860 [35]. The veins were described as brecciated and as bearing galena, sphalerite, chalcopyrite, pyrite and barytes. Some attempt at exploitation is implicit in the comment that the fractured nature of the vein renders mining a hazardous activity. The area next received attention during a resurgence of exploration activity in the 1970s and 1980s, during which time regional stream sediment sampling undertaken by Consolidated Gold Fields identified anomalous gold in the vicinity of Lead Trial. Information describing this work remains proprietary, but data sets were subsequently obtained by GreenOre gold following the acquisition of the exploration license in 2017. Although visible gold was observed in the mineralized outcrop, rock chip sampling by Consolidated Gold Fields yielded disappointing results with maximum grades of around 1 ppm, although subsequent exploration by Colby Resources in 1990 yielded higher gold grades (2.8 ppm) in galena-rich vein material [36].

2.4. Regional Gold Metallogeny Deduced from Previous Gold Compositional Studies

Gold compositional studies of alluvial gold in the Loch Tay region [2] identified two broad signatures. Gold occurrences hosted by Dalradian metasediments exhibited a high (10–40 wt%) Ag range with detectable Hg at some localities. The inclusion suite comprised pyrite and other simple sulphides such as galena, chalcopyrite and sphalerite. In contrast, alluvial gold from occurrences close to the Comrie Pluton yielded a more complex mineralogical inclusions signature including bismuth telluride, bornite and molybdenite, strongly suggestive of magmatic hydrothermal regimes [37]. The nature of mineralizing fluids responsible for metasediment-hosted gold remains unclear, but contributions from magmatic fluids [29,34] and mantle-derived fluids [38] have been proposed.

3. Materials and Methods

3.1. Commercial Exploration and Parallel Postgraduate Studies

GreenOre Gold, Erris Gold Resources and Green Glen Minerals were active over a four-year period between 2017 and 2021, during which time the Lead Trial occurrence and the adjoining north side of the Ardtalnaig valley were systematically explored using classical field prospecting, lithogeochemistry, soil geochemistry and a ground-based magnetic survey. Drill targets were identified, and reconnaissance drilling generated 584 m of core from 6 holes. Outcomes from the various exploration approaches are summarized in the following section. The exploration program was undertaken in parallel to three postgraduate projects. Each of these projects involved independent petrographic studies applied to different contexts: i. with respect to other examples of regional gold occurrences [39], ii. with respect to wider regional metallogenic studies [40] and iii. with respect to drilling results [41]. These studies made use of standard approaches to characterization of vein material using petrography and scanning electron microscope (SEM) imaging. The cathodoluminescence facility of a Tescan Vega 3 XM (Tescan, Brno, Czech) was used to characterize vein paragenesis according to quartz generations.

3.2. Gold Compositional Study

Our gold particle study was undertaken in parallel with the exploration program, following the methodologies previously described [42]. A total of 706 gold particles from six localities contributed to the study, four of which were alluvial samples and two consisted of gold recovered from crushed mineralized material. The details of sample locations are presented in Table 1 and Figure 1B, together with measures of overall abundance, heterogeneity and abundance of inclusions.

Table 1. Details of particulate gold samples. Localities depicted in Figure 1A. * 203 particles were subject to alloy analysis with a further 147 being examined for inclusions only. n.d. = not determined.

Sample Type	Sample Name	Grid Reference	No. Particles	% Particles Showing Complex Microfabrics	% of Particles Containing Inclusions
Alluvial	Ardtalnaig 1	NN 72470 38585	52	n.d.	13
Alluvial	Ardtalnaig 2	NN 71843 38594	252	82	10
Alluvial	Ardtalnaig 3	NN 72708 38029	4	n.d.	0
Alluvial	Ardtalnaig 4	NN 72960 38953	1	0	0
In situ	Lead Trial	NN 70838 39250	350 *	82	45
In situ	Tullichglass	NN 72669 38546	48	77	0

Approaches to the collection of gold particles varied according to the location. For in situ samples, gold particles were panned directly from spoil at Lead Trial following hand screening of crushed dump material at 1 cm. A > 1 m mineralized boulder at Tullichglass is almost certainly proximal to its original setting and is considered an 'in situ' sample for the purposes of this study. Vein material from the Tullichglass boulder was crushed on site using a 'Dolly' to <1 cm and panned to obtain gold particles for subsequent study.

Populations of alluvial gold particles were collected using established specialized field techniques [43] from four localities along Ardtalnaig Burn (Figure 1B and Table 1). Alluvial gold is present along the lower reaches of the Ardtalnaig Burn from Tullichglass to the estuary at Milton (Figure 1B); however, access to the lower reaches of the burn for sampling is often problematic and hazardous due to the valley gradient and associated gorges and waterfalls. Whilst gold was recovered from two outlying sites (Ardtalnaig 3 and 4,

Figure 1B), the abundance was extremely low (Table 1). Considerable effort was invested in obtaining the sample Ardtalnaig 2, as gold was scarce even in favorable collection sites. The sample Ardtalnaig 1 was collected from a 50 m stretch within a region of relatively shallow gradient affording access to well-established gravel bars.

Gold particles were mounted, set in resin, and polished according to the standard workflow [42] comprising inspection with a FEI Quanta 650 FEG-SEM (Thermo Fisher Scientific, Waltham, MA, USA), to characterize alloy microfabrics using backscattered electron (BSE) imaging. Inclusions were identified using an energy-dispersive X-ray spectroscopy system of the SEM. The analytical approach to alloy analysis using electron probe microanalysis (EPMA) has been described previously [42] and involves the determination of Au, Ag, Cu, Hg and Pd using a Joel 8230 superprobe (JEOL Ltd., Tokyo, Japan). Detection limits for Cu, Pd and Hg are c. 200 ppm, 200 ppm and 1800 ppm, respectively. Establishing the Ag profiles of a population of gold particles where individuals are commonly heterogeneous is achieved by analysis of what is interpreted to be the initial stage of alloy emplacement [42]. Identification of the primary alloy is achieved through the interpretation of the spatial arrangement of different alloys in BSE imaging mode. In some cases, additional analyses characterized multiple alloy compositions within individual particles.

4. Results

4.1. Commercial Exploration

4.1.1. Vein Mineralogy at Lead Trial and Tullichglass

The auriferous lead–zinc veins hosted in schist show complex textures with variably brecciated, vuggy, and sheeted domains. Sheeted domains tend to be located within the core of the vein (Figure 2A). The brecciated and vuggy textures (Figure 2B) are typically confined to vein margins and their immediate host rock. In both cases, different generations of quartz are clearly visible. The wall rock is heavily altered, showing strong chloritic (propylitic) alteration of the schist and argillic alteration of the felsic metavolcanics. All rocks are heavily silicified (phyllic alteration). Pyrite is present as a component of wall rock fragments hosted by brecciated veins (Figure 2C) rather than as part of the quartz vein–sulphide paragenesis, which comprises coarse galena and Fe-poor sphalerite up to 2 cm in size (Figure 2D). Minor chalcopyrite has also been observed in this main sulphide stage. Gold particles to around 100 µm have been observed to be closely associated with galena (Figure 2E) within quartz (Figure 2F) and also as particles lining vugs [39–41]. A late stage of mineralization comprising barytes and carbonates appears widespread.

The mineralized boulder at Tullichglass (Figure 2G) is texturally very similar to the Lead Trial veins containing vuggy mineralized veins but lacks the metavolcanic host rock. The veins comprise both clear, sugary quartz and iron-stained quartz that host galena particles up to 5 mm in diameter (Figure 2H). Fe-poor sphalerite is present, but it is far less abundant than galena.

None of the postgraduate studies had the opportunity to systematically characterize multiple examples of mineralized material from throughout the LTVA. Similarly, given the complexity of vein evolution and the scale of textures within them (with respect to the size of standard thin sections), the generation of a comprehensive paragenetic sequence for Lead Trial and other veins was not feasible. Nevertheless, all studies identified multiple generations of quartz but differed in terms of timing ascribed to Pb-Zn-Au emplacement within the overall quartz paragenesis, probably reflecting the differences in timing of fracturing and the number of opening-sealing cycles. Several detailed observations provide important insights at a small scale. Firstly, whilst some vugs survive, others contain an infill of fine crystalline quartz [39,41]. Gold, sphalerite and galena have all been observed lining vugs (both preserved and infilled [39,40], but these minerals may not necessarily represent the last stage of mineralization if the vug remained intact during subsequent quartz addition. The textures of multiple early quartz stages were described via cathodoluminescence studies [39], and detailed observations of the relationships between truncated quartz textures and infill were interpreted as evidence for fluctuating conditions of mineralization, including periods of quartz dissolution. Petrographic studies [39–41] returned similar vein mineralogy to that observed in hand specimens comprising galena and sphalerite, with minor chalcopyrite and pyrite.

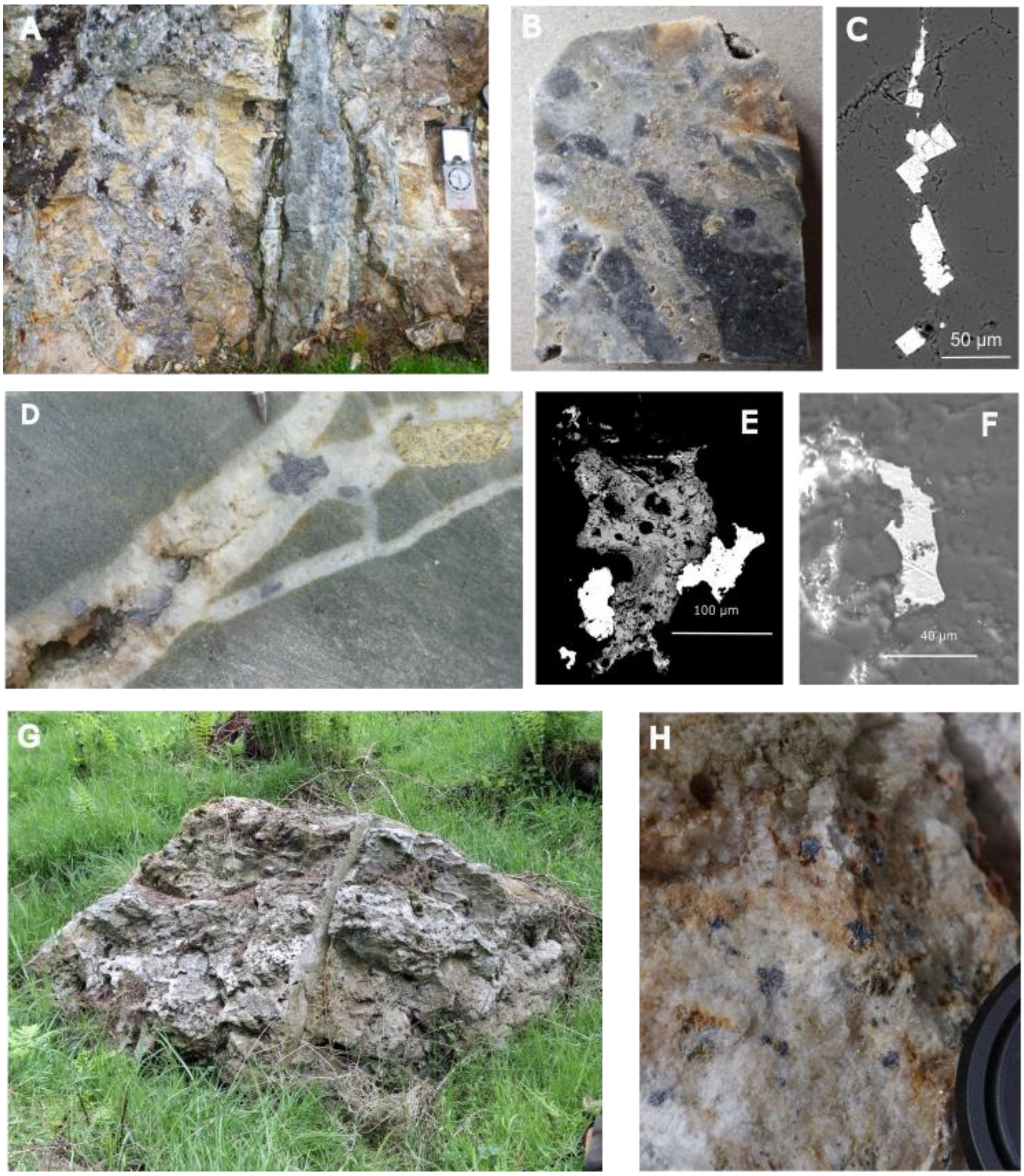

Figure 2. Mineralized material and ore textures from Lead Trial (**A**–**F**) and Tullichglass (**G**,**H**). (**A**): Outcropping quartz vein at Lead Trial showing brecciated and vuggy vein margins with a core of sheeted texture. (**B**): Brecciated vein incorporating heavily silicified wallrock clasts. (**C**): Pyrite hosted by an altered wallrock clast within a brecciated vein. (**D**): Galena-bearing vein in core from Lead Trial. (**E**): Gold particles adjacent to galena. (**F**): Gold particle hosted by quartz. (**G**): Float Boulder showing site of channel sampling and chip sampling. (**H**): Detail of vein mineralization showing galena to 1 cm hosted in quartz.

4.1.2. Other Exploration Methods

A summary of activities and major findings of the recent research program is provided in Table 2, and they are linked to the images presented in Figure 3.

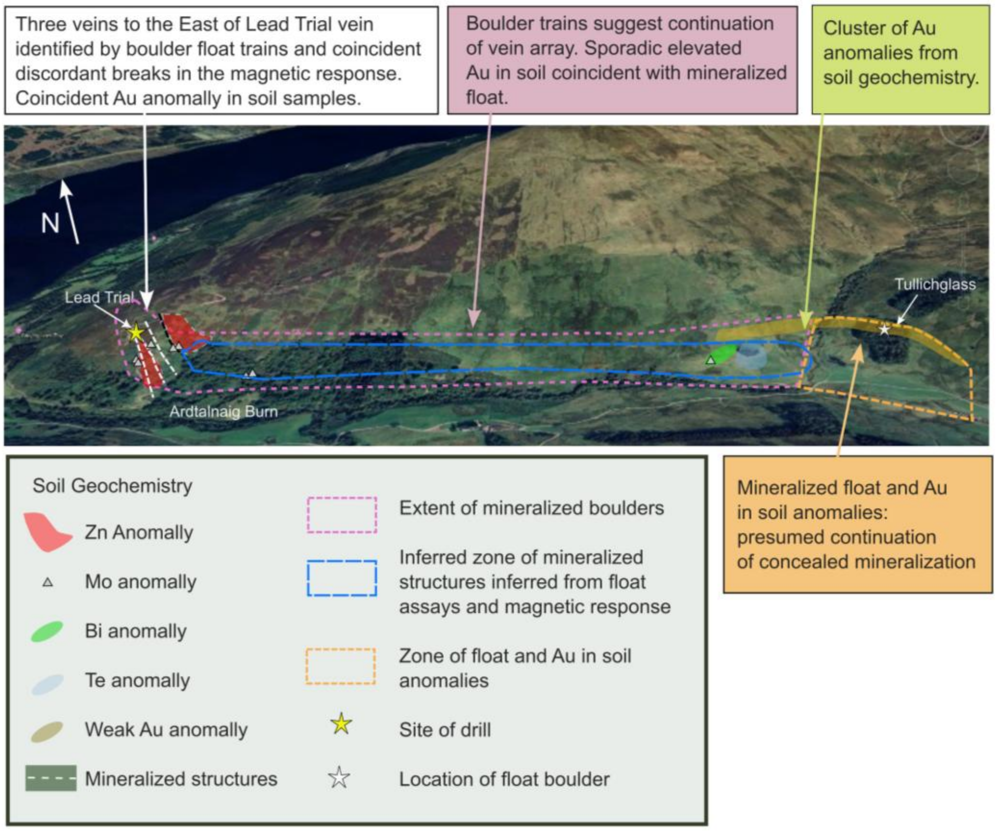

Figure 3. Major findings of the exploration campaign over the LTVA. Google Earth image, date: 4 April 2025, image location 56°31′26″ N, 4°05′68″ W, elev. 283 m, eye alt 1.14 km.

Exploration in the study area focused on the environs of the vein at Lead Trial in the West and around Tullichglass in the East (Figure 3). At Lead Trial, channel sampling of the vein returned very variable Au values, with individual grades of up to 15.4 g/t, and an average grade of 2.8 g/t over 0.8 m recorded at different sampling points. The presence of three nearby additional veins, around 50 m apart, was inferred by linear arrays of large (to about 20 tonnes) mineralized boulders, coincident with discordant magnetic responses. Sampling of mineralized boulders returned similar grades: for example, 4.52 g/t over 0.8 m and 3.11 g/t over 0.95 m.

A second zone of anomalous Au values in boulder-sized float was identified in the environs of Tullichglass (Figure 3), where grab sample grades up to 17.15 g/t and 14.85 g/t over 80 cm were recorded. Float trains yielding individual samples returning up to 16.45 g/t and weaker magnetic responses suggested further concealed veins between Lead Trial and Tullichglass, delineating a mineralized area of 4.5 km^2. Most mineralized samples exhibited Au-Pb-Zn-Hg-Mo signatures, but Cu-Bi-Te-bearing mineralization was observed in a float clast in the SE of the area.

Soil geochemistry identified a gold anomaly in the environs of outcropping veins at Lead Trial, coincident with a very strong Zn response. Zinc was present throughout the study area but at lower concentrations. Gold anomalies in soil were sporadic for about a kilometer east of Lead Trial before rising in the vicinity of Tullichglass. A cluster of minor anomalies for Bi, Te and Mo was identified to the west of Tullichglass, downslope from a 300 m long narrow gold anomaly of moderate gold concentration (Figure 3).

Synthesis of geochemical data from sampling rock chips, cut channels, and soils, together with a ground-based magnetic survey, permitted the location of drill targets for a small exploratory campaign. Although sub-surface mineralization of the target type was identified during the scout drill program (1.65 m at 4.44 g/t), post-mineralization faulting has prevented further characterization of the ore body, and further drilling is required.

The textures of quartz veins recorded in outcrop at Lead Trial and in float across the whole LTVA appear consistent, comprising multi-generational sugary vein quartz often showing a vuggy and/or brecciated texture. The proportions of galena and sphalerite appear to vary, with the abundance of sphalerite decreasing to the east of Lead Trial: an observation that accords with the location of the Zn soil anomaly. Chalcopyrite is a minor constituent and often appears to be associated with galena [40,41]. Gold particles recovered from the dumps at Lead Trial and from the float at Tullichglass were mostly around 50–100 μm in size, and it seems likely that other gold occurrences throughout the LTVA would yield gold of a similar size. Consequently, both irregular Au assays from lithogeochemical studies and the spatial variability in the gold assays from soil sampling may result from the nugget effect. Paragenetic sequences within veins may be complex and almost certainly include more than one stage of emplacement of galena, sphalerite and gold. In addition, cathodoluminescence (CL) studies identified complex textural relationships both within and between different generations of quartz, interpreted to indicate fluctuating conditions in the hydrothermal system [39].

Table 2. Summary of recent exploration activities.

Technique	Summary	Outcomes
Field prospecting	Initial focus on the Lead Trial occurrence, where the major vein system crops out over tens of m along strike. Mineralized clasts and boulders visually similar to mineralization at Lead Trial proved relatively abundant throughout the study area, particularly around Tullichglass.	Characterization of in situ vein at Lead Trial up to 2 m in width. (e.g., Figure 2G). Mineralized boulders and other mineralized float forming linear arrays indicative of three subcropping veins immediately to the southeast of Lead Trial at approximately 50 m intervals (Figure 3). Mineralized boulders present throughout study area with a high concentration of relatively high-grade assays recorded near Tullichglass. Overall mineralized area is 4.5 km^2.
Lithogeochemistry	Rock chip sampling of both outcrop and float was undertaken to indicate the distribution of gold and other elements. (Figure 4A). Targeted channel samples were collected from both float and outcrop using a portable diamond saw to access vein material. One vein exhibiting elevated Cu, Bi-Te and As was exposed in the bed of the Ardtalnaig Burn.	Rock chip samples: multi-element analysis with Au values > 0.2 g/t and positive correlations: (Au-Hg), Au-Mo-Pb) and (Au-Ag). Channel sampling: presence of visible gold confirmed in the vein quartz, but distribution was irregular. Assays variable due to nugget effect, but grades of 8–17 g/t Au regularly recorded. Vein analysis suggests Bi telluride, chalcopyrite-arsenopyrite/cobaltiferous gersdorffite assemblage. Gold values were very low (0.23 ppm) and the sample was not retained for further study.
Soil Geochemistry	Sampling focused on the area to the south of Lead Trial and in the environs of Tullichglass.	Au anomalies were often spatially sympathetic to the locations of high-grade boulders. Zinc anomalies were present throughout, but highly elevated adjacent to Lead Trial (Figure 3). Lead values were consistently elevated over the whole study area and Hg was sporadic. Mo, Bi and Te exhibited sporadic anomalies but clustered at and to the east of Tullichglass (Figure 3).
Magnetic survey	A ground-based geophysical survey using a portable magnetometer was undertaken mainly to identify structures and any anomalous areas of magnetic response resulting from hydrothermal alteration associated with the mineralizing process.	Weak magnetic anomalies spatially coincided with the vein observed in outcrop at Lead Trial, and three others correlated with mineralized boulder trains identified by field prospecting. Magnetic responses between Lead trial and Tullichglass suggest mineralized structures sympathetic to float trails (Figure 3).

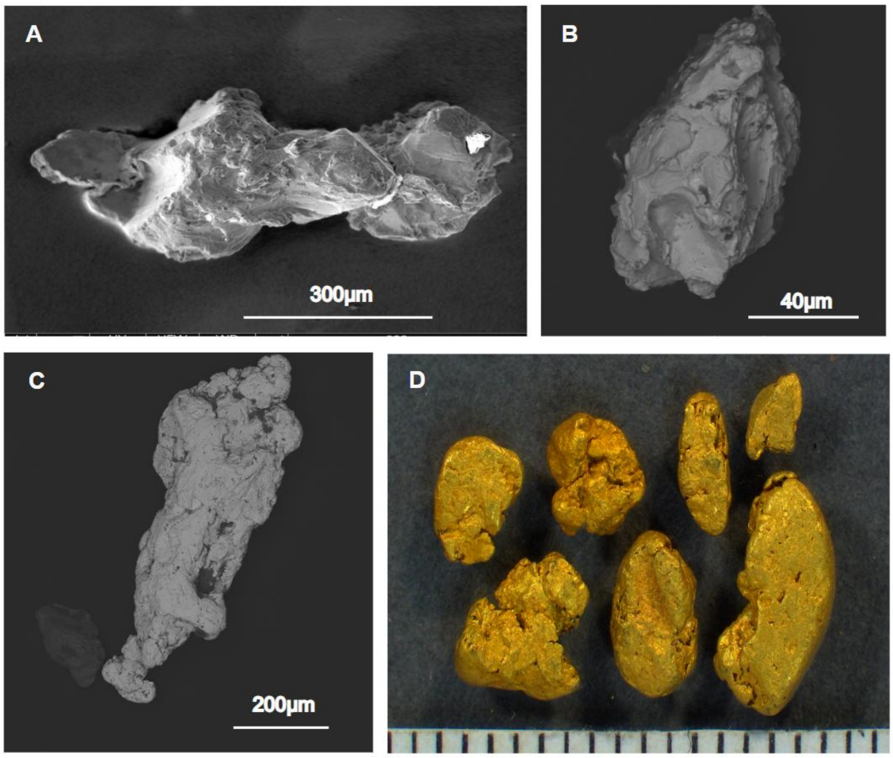

Figure 4. Examples of in situ and placer gold from the LTVA. (**A**–**C**): SE images. (**A**): Particle panned from the dumps at Lead Trial. (**B**): Particle panned from crushed vein material, Tullichglass. (**C**): Small, rough placer particle from Ardtalnaig burn. (D): Coarse alluvial gold particle from Ardtalnaig Burn.

4.2. Gold Particle Study

4.2.1. Size and Morphology of Gold Particles

Gold particles were abundant in the dump material at Lead Trial; most were 200–400 µm in the longest dimension, with the largest recovered being about 1 mm (Figure 4A). Gold recovered from crushed ore at Tullichglass was smaller, with most particles around 100 µm (Figure 4B). Alluvial particles from Ardtalnaig 1 and 2 showed a bimodal distribution of size and morphology. Most were between 100 µm and 1 mm in length and rough (e.g., Figure 4C) but a few were much larger, attaining 6 mm in length (Figure 4D). These particles also exhibited some hackly surfaces and attached quartz.

4.2.2. Gold Alloy Signatures

The number of gold particles recovered from sites Ardtalnaig 3 and Ardtalnaig 4 is too small to permit characterization of those populations and is not considered further. Figure 5A shows the Ag profiles of the four sample populations under consideration. For heterogeneous particles (i.e., where BSE imaging shows evidence of partial modification of the alloy composition by later fluids), the analysis point corresponds to what is interpreted to be the earliest alloy composition.

The Ag contents of all gold alloys fall into four distinct groups, identified by continuous compositional ranges separated by breaks in the slope. These ranges are henceforward referred to as Alloys A–D, where Alloy A is the range of lowest Ag values and Alloy D is the highest (Figure 5A).

Alloy A comprises gold particles containing between 4 and 16 wt.% Ag. With one exception, these are all derived from alluvial sample populations. Alloy B (16–23 wt.% Ag) was observed only in alluvial gold particles. Alloy C (23–32 wt.% Ag) is the major component of gold from Lead Trial and Tullichglass but also forms an important subpopulation in each of the alluvial sample populations. The compositional range of Alloy D is relatively high (32–60 wt.% Ag) and includes populations from all sampling localities.

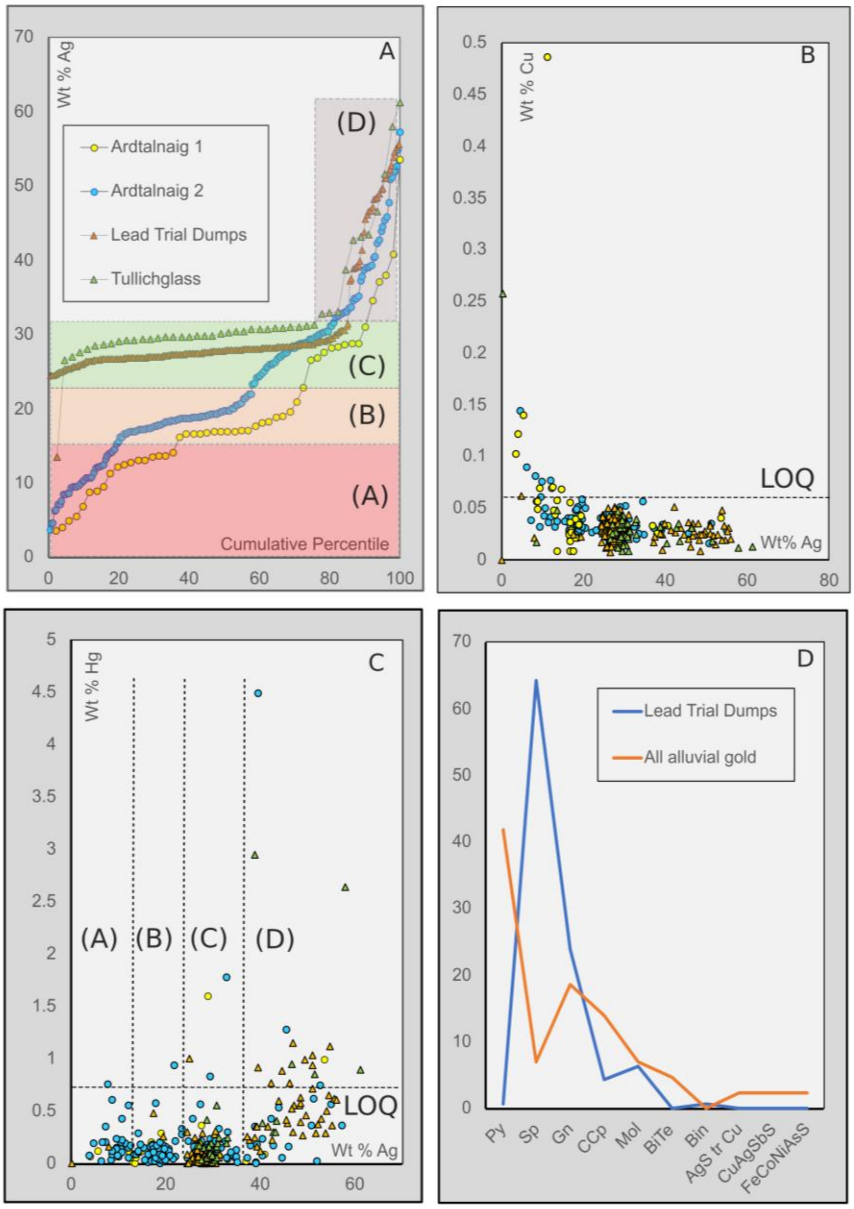

Figure 5. (**A**): Ag profiles of gold particles from alluvial and in situ localities. The significance of areas labeled A–D is discussed in the text. (**B**): Covariance of Ag and Cu. (**C**): Covariance of Ag and Hg. (**D**): Inclusion suites of gold from Lead Trial and alluvial samples. Data points refer to the proportion of particles that exhibit a specific mineral in section with respect to the total number of inclusion-bearing particles. 'LOQ' = 'limit of quantitation'.

Palladium values were below LOD in all cases and are not considered further. Almost all Cu values are below the limit of quantitation, but all measurable levels of Cu occur within Alloy A, where Cu and Ag broadly correlate inversely (Figure 5B).

The data that generate the Ag profiles and the Cu-Ag plot comprise one data point representing the first alloy composition within every gold particle. In some cases, multiple analyses were undertaken of the same particle to establish compositional variation exhibited by heterogeneous microfabrics. The Hg-Ag bivariate plot shown in Figure 5C has used all data available, i.e., analyses of multiple alloy compositions within heterogeneous particles have been included. This approach has been adopted to illustrate the range of Ag-Hg compositions in the Au alloy, but it does not reflect the overall abundance of different Au-Ag-Hg alloys because alloy compositions often grade into each other (e.g., Figure 6A–C,G–I,L), and not all heterogeneous particles have been subject to multiple analyses. Measurable Hg is largely confined to Alloy D but almost all Alloy C contains detectable Hg.

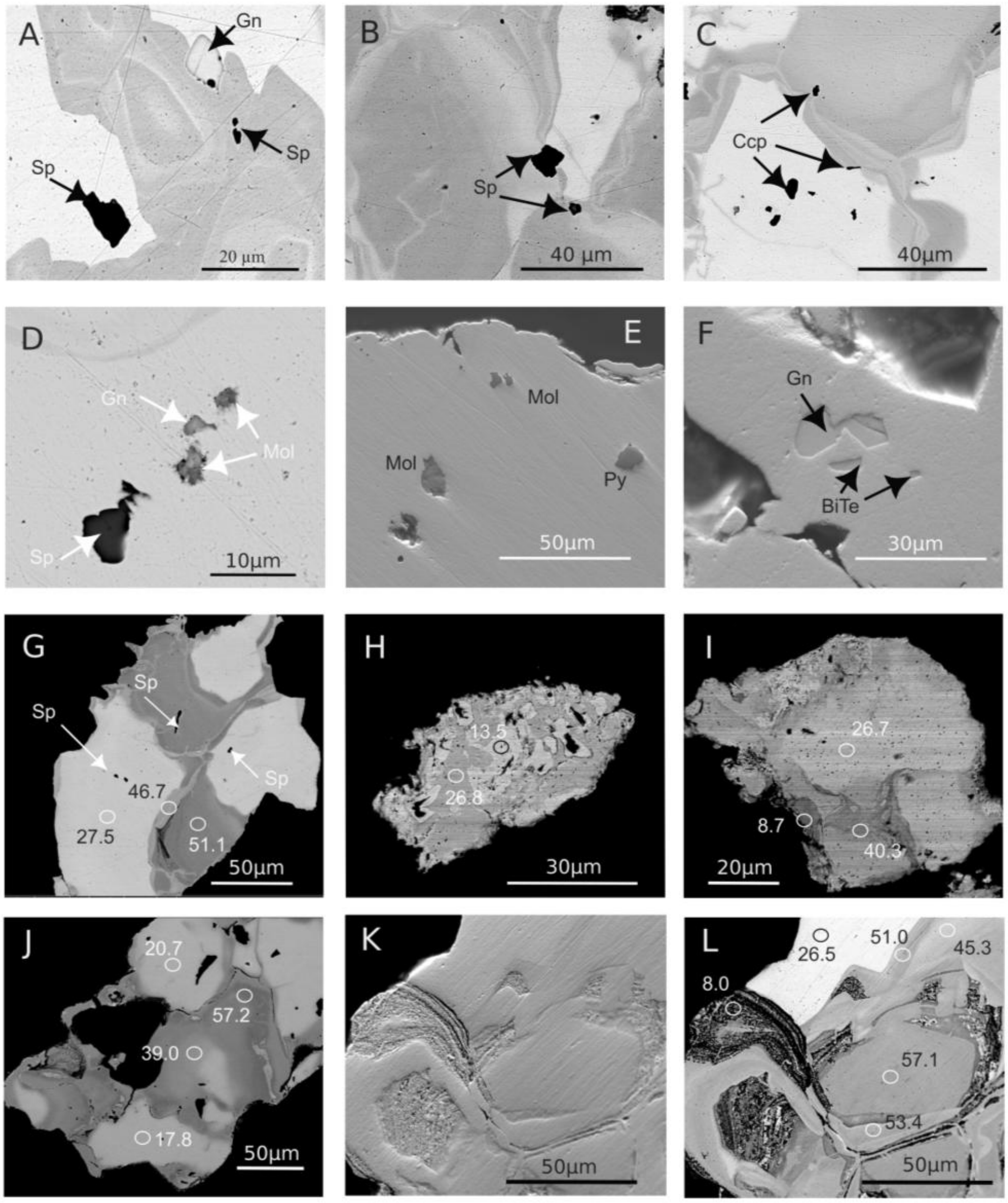

Figure 6. Heterogeneity in gold particles, alloys and inclusions in the studied samples. (**A**–**D**,**G**,**K**,**L**): Lead Trial; (**E**,**F**,**J**): Ardtalnaig Burn. (**H**,**I**): Tullichglass. (**A**–**C**): inclusions within different alloys and at their interfaces; (**D**): coeval galena, sphalerite and molybdenite; (**E**,**F**): examples of associations of Bi and Mo mineral inclusions. (**G**): Clear relationships between primary alloy, altered alloy and crosscutting late alloy. (**H**): Co-existence of Alloy A and Alloy C (see Figure 5A). (**I**): Diffuse boundaries between gold of 26.7 wt.% Ag (Alloy C) and 40.3 wt.% Ag (Alloy D) and porous gold of 8.7 wt.% Ag at margin. (**L**): Alloy C showing heterogeneous alteration to Alloy D. (**J**–**L**): particles from Ardtalnaig Burn. (**J**–**L**): Pair of images of the same target showing recessed areas in (**K**) corresponding to lower Ag values in (**L**). (**L**): Particle showing 4 stages of alloy development and emplacement: primary alloy (26.5 wt.% Ag), Ag enhanced alloy (values 51.0, 45.3, 57.1 all wt.% Ag), Ag leached from alloy (8.0 wt.% Ag), late crosscutting stage (53.4 wt.% Ag). (**K**) is an SE image; all others are BSE images. IMA-CNMNC-approved mineral symbols are used throughout [44].

4.2.3. Inclusion Signatures

Inclusions were observed in 45% of the gold particle sections from Lead Trial, but none were observed in the sample population of 48 particles from Tullichglass. Examples of sphalerite and galena inclusions in gold from Lead Trial are provided in Figure 6A,B where they may be situated in either Alloy C or D. Inclusions are observed both within the earliest alloy and at the interface of this alloy with a more Ag-rich alloy (Figure 6A–C). Chalcopyrite inclusions are far less common but may also reside within different gold alloys within a single particle (Figure 6C). Molybdenite inclusions were observed in the same gold particles as sphalerite and galena (Figure 6D). Pyrite and galena are both common inclusions in gold from Ardtalnaig Burn, and Figure 6E,F show inclusions of molybdenite with pyrite and galena with an undifferentiated Bi telluride, respectively.

The inclusion data are illustrated in Figure 5D. For the purposes of diagrams, the inclusion suites of the two alluvial gold populations have been combined because i. there is insufficient data to permit meaningful interpretation of the data set from Ardtalnaig 1, ii. The Ag profiles of the two sample populations are almost the same (Figure 5A), strongly suggesting that both populations are derived from the same type of source (or the same combination of individual sources). Inclusion signatures may be characterized either on the basis of the proportions of inclusion-bearing particles that contain a specific mineral species or overall chemistry of the inclusion suite [4,37]. In the present study, a mineralogical approach using spider diagrams has provided a clearer indication of key differences between sample populations. The signature of the gold from Lead Trial differs from that of alluvial gold by the dramatically different contributions from pyrite (almost absent in in situ gold from Lead Trial) and sphalerite (very rare in the alluvial inclusion suite) (Figure 5D). Molybdenite, galena and chalcopyrite were recorded in broadly equivalent proportions in each. Bismuth telluride inclusions were observed in two alluvial particles but not in gold from Lead Trial, although a Bi-sulphide inclusion was recorded. There are minor contributions from sulpharsenides and sulphosalts in the inclusion suite of alluvial gold.

4.2.4. Microfabrics of Gold Particles

Alloy C forms the homogenous part(s) of in situ gold particles from Lead Trial (Figure 6A), but around 80% of the sections of gold particles exhibited microfabrics in which Alloy C has been altered to Alloy D (e.g., Figure 6A–C,G–J). These patches of Alloy D are usually internally heterogeneous with respect to their silver contents and may contain detectable Hg to a maximum of 1.15 wt.%.

Figure 6K,L show images of the same sample using secondary electron and BSE modes, respectively. The SE imaging shows recessed porous areas that appear dark when viewed in BSE imaging, even though this Au alloy contains much lower concentrations of Ag than any of the other alloys. In some cases, the shape of the porous zone is sympathetic to that of boundaries between other adjacent alloys of different Ag contents (Figure 6L). The homogenous Au-Ag alloys, the heterogeneous Au-Ag alloys and the porous zones may be either cut or truncated by a later Au-Ag alloy (Figure 6L). Inclusions were observed within the gold of all alloy categories and at their interface. where the geometry of the contact between different alloy types is usually influenced by their presence (Figure 6A–C).

Gold particles from Tullichglass exhibited similarly heterogeneous microfabrics in around 80% of cases (Table 1), with both sharp and diffuse boundaries separating alloys of compositions corresponding to Alloys C and D (Figure 6H,I). In addition, the porous texture comprising a relatively high Au alloy was observed. One particle comprised a small sub-particle of Alloy A in sharp contact with Alloy C (Figure 6H).

Alluvial gold particles collected in Ardtalnaig Burn are also commonly heterogeneous with respect to Au-Ag alloys (Figure 6J). The nature of heterogeneous microfabrics is similar to that observed in gold from the in situ localities, with both sharp and diffuse contacts between different alloys, and commonly patches of Alloy B that exhibit compositional zonation into Alloys C and D (Figure 6J). The proportion of particles that exhibit alloy heterogeneity varies according to compositional zone and was 17%, 45%, 33% and 21% for Alloy A–D, respectively.

5. Discussion

5.1. Outcomes from the Gold Compositional Study

5.1.1. Alluvial-In Situ Gold Relationships

Alluvial gold particles were far more abundant at Ardtalnaig 2 than farther upstream at Ardtalnaig 1, in broadly equivalent fluvial settings. This suggests that gold enters the Burn between sites, rather than being dispersed from a single source upstream of Ardtalnaig 1. This hypothesis is consistent with the rough morphologies of gold particles at both sites (Figure 4), suggestive of very limited fluvial transport. Gold from Lead Trial would not be expected to contribute to the alluvial samples that were collected several hundred meters upstream of the projected outcrop of the Lead Trial vein on the valley floor. The genetic relationships between the two alluvial samples and the mineralization observed in the float boulder at Tullichglass may be inferred from the Ag profiles illustrated in Figure 5A. Both alluvial populations exhibit the same distinctive compositional ranges and in the same proportions. Therefore, the compositional range of gold entering the fluvial system is the same over several hundred meters. One of these compositional ranges is almost certainly sourced from gold mineralization of the type present at Tullichglass because of the near identical Ag ranges. Despite the fact that only one gold particle from the Tullichglass boulder contains alloy A, this result indicates a potential genetic link between the mineralized boulder and a subpopulation of the alluvial gold.

Gold from the in situ localities of Lead Trial and Tullichglass exhibits very similar Ag profiles, dominated by Alloy C (Figure 5A), but sphalerite appears more common in the veins at Lead Trial, where it also constitutes a major component of the inclusion suite within gold particles (Figure 5D). On the basis of inclusion suites, the alluvial samples cannot be sourced from gold of the Lead Trial signature, but a genetic association with the Tullichglass type (as inferred from alloy compatibility) is feasible, as the absence of inclusions in gold particles liberated from the Tullichglass boulder is not evidence for their complete absence in gold of this type.

Neither Alloy B nor the Au-pyrite association of the inclusion suites present in the alluvial samples may be correlated with any in situ mineralization identified to date. Whilst pyrite has been recorded at Lead Trial (Figure 2C), it is hosted by silicified wall clasts and is not observed to be coeval with gold. The dominant host rock lithology at Lead Trial (felsic metavolcanic) differs from the metasedimentary lithology elsewhere, but at present, we are unable to assess how much this may have played a role in the mineralogical differences. Either way, the presence of Alloy B in the alluvial sample populations is a clear indication of a gold mineralization type that has not to date been identified in situ.

It is of interest to note that the particle size range of the alluvial gold includes nuggets up to 0.6 g (Figure 4D), i.e., substantially larger than the maximum size observed either in dump material at Lead Trial or during visual inspections of float. Individual gold particles are not measured prior to analysis, but they are mounted according to size range. Consequently, it is possible to evaluate whether there is broad covariance between particle size and alloy type, but no such relationship was observed and therefore it seems probable that larger gold particles are present in the vein material but have yet to be observed because of their relative rarity.

5.1.2. Relationship Between Gold Alloy Compositions, Microfabrics, Inclusion Suites and Vein Paragenesis

Heterogeneous gold particles were observed in all sample populations of gold particles. The nature of the heterogeneity and the textural relations between different heterogeneous microfabrics may be interpreted to aid understanding of the evolution of the hydrothermal system.

Characteristics of heterogeneous gold particles such as those depicted in Figure 6 have been synthesized in a schematic diagram (Figure 7) to illustrate the sequence of events that have generated the interrelationship of observed microfabrics. These stages of gold emplacement and/or modification are described below.

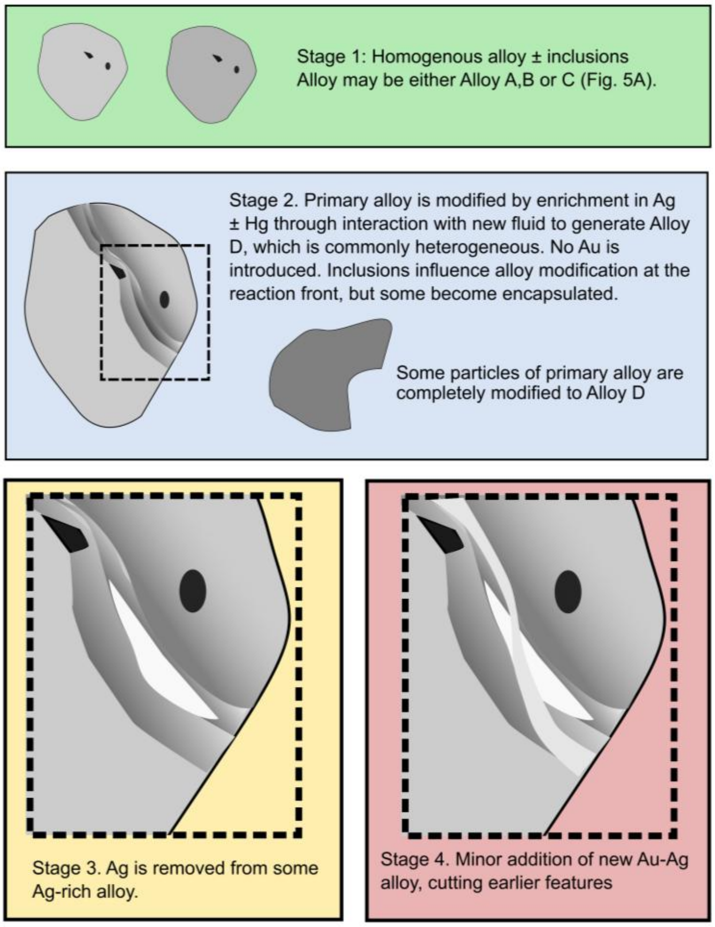

Figure 7. Schematic diagram showing the emplacement and modification of gold particles during the evolution of the hydrothermal system. Greyscales have been chosen to represent textures observed in BSE mode in Figure 6, except in stage 4, where the new alloy is shown as pale gray for clarity.

Stage 1 comprises the first gold alloy to precipitate. Three Ag ranges of primary gold have been observed, corresponding to gold compositions Alloy A–C in Figure 5. Alloy types A and B are not present at Lead Trial, so they only precipitate at localities in the upper reaches of Ardtalnaig Burn, although Alloy B is not observed in situ at Tullichglass. Alloy C is present at all sampling localities. Primary gold is homogeneous irrespective of Ag content and hosts a range of mineral inclusions.

Primary gold alloy is often accompanied by patches of Alloy D, which itself may be highly heterogeneous (Figure 6A–C,G,I,J,L). Boundaries between primary gold and Alloy D may be sharp (Figure 6A–C,G,H) or diffuse (Figure 6I,J). Inclusions situated at the interface between the primary alloy and Alloy D distort the line of contact (Figure 6A–C). Heterogeneity within Alloy D may comprise subparallel zones of different alloy compositions. Individual zones may contain a homogenous alloy or exhibit a compositional gradient (e.g., different areas depicted in Figure 6A–C). In some cases, the pattern of alloy variation is sympathetic to 120° angles, showing that heterogeneity is likely to be a consequence of grain boundary migration (e.g., Figure 6A,C) [42]. In other cases, irregular areas of Alloy D exhibit diffuse contacts with the primary alloy. All these textures are consistent with the modification of pre-existing gold by a fluid not in equilibrium with the primary alloy rather than the addition of new gold [42]. The frequent observation of the same inclusion species in primary alloy in adjacent patches of Alloy D and at their distorted contact provides evidence for alloy modification by a progressing reaction front, impeded in the vicinity of the inclusion (Figure 6A–C). Collectively, these modifications are ascribed to a second stage within the evolution of the hydrothermal system, in which local and probably transient conditions have modified the primary alloy composition without adding new gold. In some cases, particle modification has progressed to completion, where the variation in Ag content between 32 and 60 wt.% Ag provides further evidence for fluctuating conditions.

The third stage of gold particle evolution (Figure 7) involves the local removal of most of the Ag to generate a porous texture (Figure 6K,L). Porous areas are usually parallel to compositional zones in the immediate microfabric and it seems likely that they represent preferential Ag removal from zones that previously exhibited relatively high Ag contents, because such areas may be more reactive to fluids in which Ag is soluble.

Finally, there is a very minor introduction of a homogenous gold alloy of between 45 and 55 wt.% Ag that crosscuts all previous features (Figures 6G,L and 7).

To some extent, it is possible to correlate the microfabrics observed in gold particles with paragenetic interpretations of the quartz generations. Whilst the full characterization of vein paragenesis has not yet been established, it is clear that the textural variations within and between stages of quartz emplacement are compatible with pervasive modification of pre-existing gold particles. Gold particles that line preserved vugs were not susceptible to modification by later fluids, whereas those in contact with evolving fluids at the interface of two quartz generations could be expected to show evidence of full or partial re-equilibration of pre-existing alloy according to the degree of fluid–gold contact. In this hypothesis, the extent of alloy modification is controlled by the surface area of fluid contact and the duration of that contact. In particular, the observation that in some cases pre-existing quartz was dissolved [39] could be attributed to a temperature rise that would also result in preferential Ag removal from pre-existing alloy [45] (Figure 6K,L).

In conclusion, the primary gold alloys emplaced in stage 1 (Alloys A–C, Figure 5) are the only economically significant episode of gold emplacement. Gaining an understanding of their genetic relationships is important because it provides more information on the scale and nature of the hydrothermal system across the LTVA than is possible through studies of outcrop or float. In the following discussions, gold composition corresponding to Stage 2 is discussed only in regard to replication of fluid conditions across the LTVA. Conditions relating to the minor events of stages 3 and 4 are not considered further.

Gold Alloys A-C could have been formed at different locations within a single hydrothermal system, or alternatively, they may result from discrete fluid injections. Spatially, Alloy C occurs at both Tullichglass and Lead Trial. Alloys A and B are absent at Lead Trial, but there is a single example of Alloy A at Tullichglass, where it appears to predate Alloy C (Figure 6H). Alloys A and B are almost certainly derived from mineralization within the Ardtalnaig valley, whose outcrop is obscured by Quaternary sediments. In this scenario, provided that Alloys A and B are present at lower elevations, they represent mineralization emplaced at deeper levels that are responsible for Alloy C. It seems probable that they are also the earliest alloys to form (Figure 6H).

The genetic relationships between gold alloys A–C may be explored both through consideration of the shape of the Ag profiles and by synthesis of alloy compositions with their respective inclusion suites. These considerations may be examined in the context of mineralogical zonation within the LTVA. Considering the relationship between alloys A and B: their Ag profiles of gold illustrated in Figure 5A show a clear slope break, in slope but the compositional range is continuous. The compositional continuum with respect to Ag could either represent a single evolving system or different fluid episodes with overlapping Ag ranges. The inverse relationship between Cu and Ag in the alloy (Figure 5B) appears more consistent with an evolving system, and falling temperature is a plausible explanation [45,46]. An evolving system is also consistent with the proportion of the most common inclusion species, which are broadly similar and suggestive of metal precipitation from the same fluid (Figure 8A). The plots for Alloys A and B in Figure 8A differ in the presence of less common minerals such as molybdenite and Bi-telluride. Currently, it is unclear whether this observation is indicative of a fundamental difference in gold composition or a consequence of small data sets. We propose that Alloys A and B were formed in the same mineralizing event, with low Ag alloys the first to form. Alloy B forms the largest component, and the relatively shallow gradient of the Ag plot is interpreted to indicate a very similar depositional environment, perhaps resulting from a sudden temperature reduction. There was no gold mineralizing event at Lead Trial at this point, and a very limited one at Tullichglass.

The Ag profile of Alloy B does not overlap with Alloy C (Figure 5A), which suggests a separate episode of mineralization, and the onset of gold precipitation at Lead Trial, the dominant event at Tullichglass and most likely all other mineralized localities between them. This hypothesis is entirely consistent with the presence of Alloy C within the population of alluvial gold particles. Figure 8A shows broad similarities between the proportions of the major inclusion minerals in all gold alloys. We conclude that Alloy C is a discrete episode within the mineralizing system of the LTVA, dominant both at Lead Trial and in the mineralized float trains visible above the elevation limit of Quaternary cover. The similarity between the Ag ranges of Alloy C in gold from Lead Trial, Tullichglass and in the alluvial population indicates widespread replication of the same mineralizing environment along deposit strike.

On the basis of the alloy compositional ranges and their associated inclusion suites described above, gold mineralization in the LTVA may be classified according to three generic primary gold Types. Type 1 corresponds to alluvial gold of the Ag range of Alloys A and B, which also host a relatively diverse inclusion suite in comparison with Alloy C (Figure 8B). Type 2 corresponds to the Alloy C composition observed in both alluvial samples and at Tullichglass. Type 3 is confined to Lead Trial and possibly the immediate environs and exhibits the same Ag range as Type 2 gold, but sphalerite inclusions are far more common (Figure 8B). A tentative deposit model is proposed that includes the three main hydrothermal events in the LTVA, and this is depicted in Figure 9. Any proposed deposit model must be consistent with the observations that i. mineralized float is visible only at elevations above complete quaternary cover, i.e., at higher elevations than the valley floor, and ii. no mineralization containing Type 1 gold has been observed either in situ or in float. Consequently, we hypothesize that gold precipitation begins with the Au-rich, Cu-bearing gold of Type 1 (because the alloy composition is consistent with the highest temperatures of mineralization), emplaced relatively deep in the mineralizing system. Bismuth-bearing minerals are most common in this gold type (Figure 8B). The brecciated vein textures observed in float throughout the study area indicate catastrophic changes in conditions, and these could account for the transition between the deposition of Alloys A and B. The narrow Ag range of Alloy B is consistent with sudden deposition under the same conditions, such as those that could result from temperature drop due to pressure release. Types 2 and 3 gold exhibit near identical Ag ranges and either represent a discrete single stage of mineralization across the LTVA, subject to similar depositional conditions, or further deposition from the same fluid responsible for Type 1 mineralization caused by further structural failure at shallower depths. Whichever of these hypotheses is correct, the identification of molybdenite and Bi-bearing galena inclusions at Lead Trial suggests genetic commonality with the mineralizing fluids of Type 1 gold. The replication of hydrothermal regimes responsible for the deposition of Alloy C, and the subsequent widespread modification of gold particles by a pervasive fluid strongly suggests connectivity within the vein array at depth. However, in this scenario, the reasons for the high Zn levels in the environs of Lead Trial remain unclear but may indicate localized interaction of fluids with relatively Zn-rich rocks.

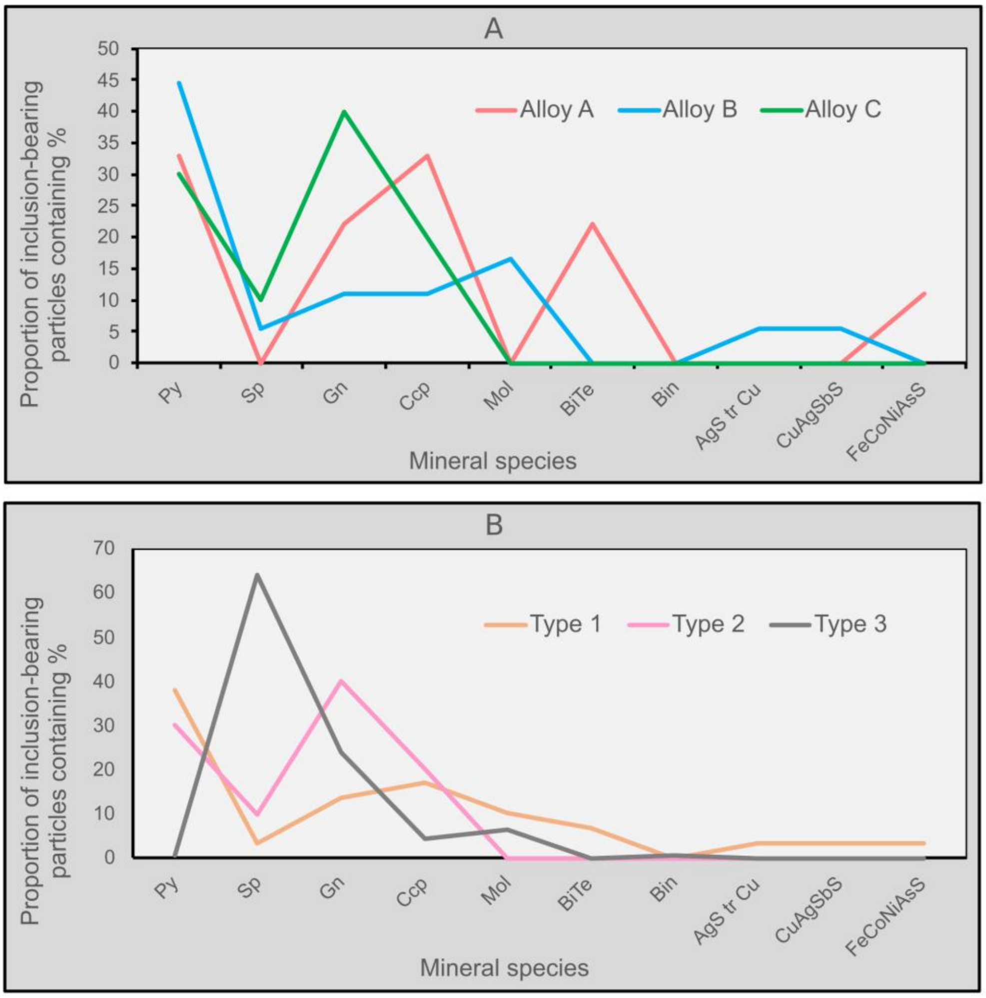

Figure 8. Inclusion signatures according to alloy compositions (**A**): inclusion suites of alluvial gold corresponding to the Ag alloy ranges defined in Figure 5A. (**B**): Inclusion signatures of gold Types identified through compositional characterization.

The pyrite-gold association, strongly evident in gold Type 1, has not yet been identified in vein or float across the LTVA. The gold-bearing mineralization at Lead Trial appears to be a Fe-poor system because of the rarity of pyrite coeval with gold and the low Fe content of the sphalerite. It may be that the importance of the Au-pyrite association increases with depth, a hypothesis supported by the pyrite quartz association noted in drill core at Lead

Trial [41]. The atypical Bi-Te-Cu bearing vein that outcropped in the stream bed 200 m above one of the alluvial sampling sites (Table 2) is a potential source of gold with the inclusion signature of Type 1, but a genetic link remains unproven. The northerly extent of the proposed zone of Type 1 gold is not known, and this is indicated in Figure 9.

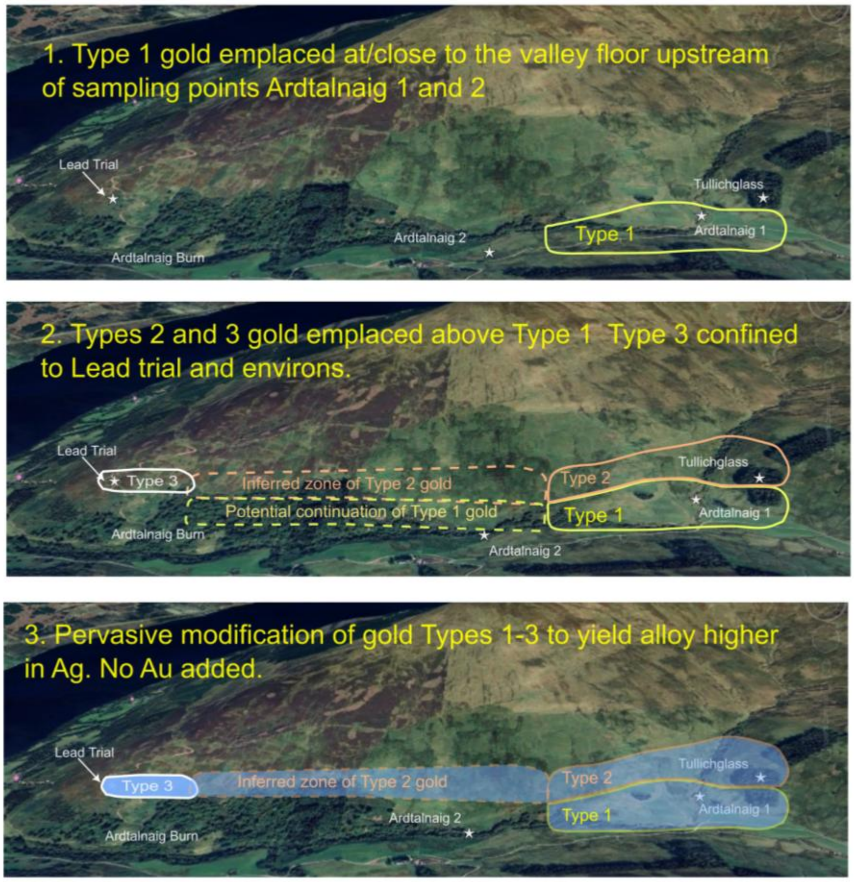

Figure 9. Geographical range of the three major stages of hydrothermal activity in the LTVA. Stages 1 and 2: gold emplacement with Type 1 deeper and earlier than Types 2 and 3. Stage 3: pervasive modification of pre-existing gold to generate an alloy richer in Ag ± Hg. Google Earth image specifications as per Figure 3.

5.1.3. Gold Particle Signature and Style of Mineralization

Several recent studies have investigated the potential of inclusion suites as diagnostic tools for determining the type of source mineralization of local and regional alluvial gold [4,37,47]. Radar diagrams depicting the chemical signature of inclusion suites according to metallic and non-metallic components have found utility as a generic format by which all inclusion signatures may be compared [37]. Whilst there may be variation between inclusion signatures of gold of the same type from different localities, general compositional templates have emerged. For example, gold from orogenic settings yields signatures that are chemically and mineralogically simpler than those for magmatic-hydrothermal systems. The inclusion suite of alluvial gold from Ardtalnaig Burn has been compared to two other regional examples of gold from magmatic hydrothermal systems: Glen Lednock and the Ochil Hills [2] (Figure 10). These alluvial populations likely contain gold from porphyry and associated epithermal systems and are notable for their wide range of component elements. The Fe-Cu-Pb-Zn-Ag-Bi association evident in gold from Ardtalnaig Burn is compatible with a magmatic origin. The non-metal signature is As-poor with respect to those of gold particles from Glen Lednock and the Ochil Hills, but worldwide other examples of gold from calc-alkaline magmatic hydrothermal systems also comprise As-poor systems.

Gold from the environs of the Casino porphyry, Yukon, and the Klaza intermediate sulphidation epithermal deposit, Yukon [37], provide examples and are compared to gold from Ardtalnaig Burn in Figure 10. Consideration of the inclusion suite of gold from Ardtalnaig Burn would have confidently predicted derivation from a magmatic hydrothermal system in the absence of any other information from exploration and academic studies.

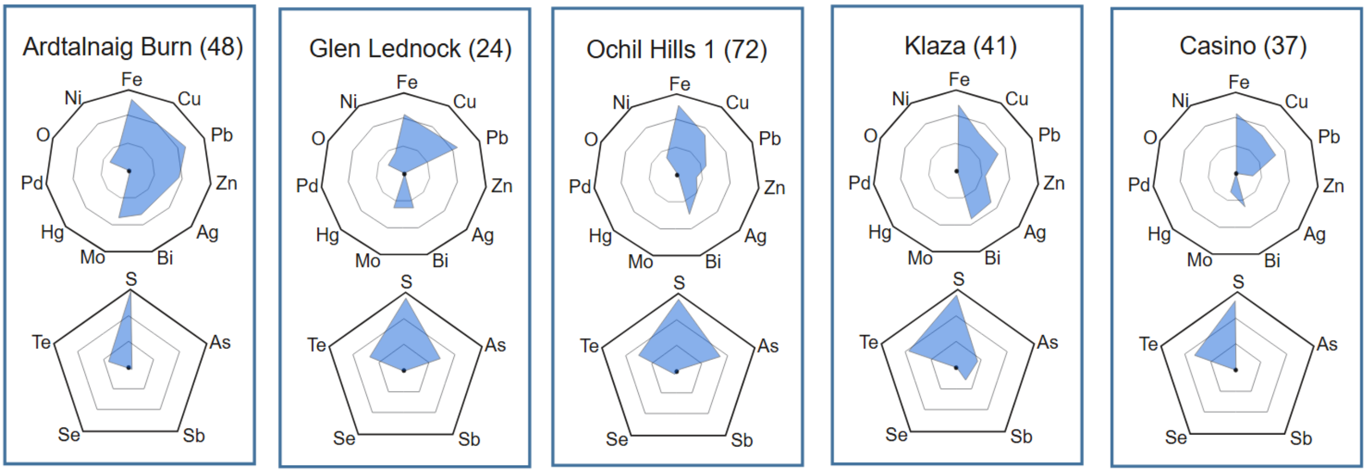

Figure 10. Comparison of the inclusion signature of gold from Ardtalnaig Burn with other examples of gold formed in magmatic hydrothermal systems.

5.2. Comparison of Outcomes from Standard Exploration and Gold Particle Studies in the LTVA

The application of gold compositional studies to the study of the LTVA has generated several outcomes that may be compared to those generated by a standard approach to exploration (Figure 11). The results of standard exploration do yield more robust outcomes with respect to data necessary for the generation of drill targets such as a clear spatial definition of outcrop and subcrop, which is not possible using gold compositional studies alone. Otherwise, exploration activities yield observations and interpretations that were wholly compatible with interpretations flowing from the gold compositional work, with the two approaches generating different levels of confidence in specific aspects of the mineralizing system. In particular, the added value of a gold particle study arises from its ability, in a relatively cost-effective way, to (i) reliably illuminate the style and extent of the wider mineralizing system; (ii) provide robust evidence of the association of gold with other minerals and elements, some of which may function as path-finders; and (iii) make predictions of the presence of mineralization whose outcrop is obscured by surface cover.

The inclusion suite observed within gold particles from Lead Trial is not only compatible with the outcome of petrographic work on vein samples but also identifies other Au-mineral associations not observed in thin sections. The mineralogy of the inclusion suites of alluvial gold is consistent with elemental anomalies observed in geochemical data, but it also provides proof of specific gold-element relationships that otherwise depend on inference from spatial coincidence. In the present study, these have been established for Au-Mo, Au-Bi, Au-Co, and Au-Hg. The similarity in compositional characteristics of gold from the two alluvial sampling sites strongly suggests unexposed source mineralization situated to the northwest of Ardtalnaig 1 and the West of Ardtalnaig 2. The anomalous concentrations of gold in soil samples in this area (Figure 3) are compatible with this hypothesis, and the adjacent soil anomalies for Bi, Mo and Te (Figure 3) are not only consistent with this model but also correlate with the inclusion signature of Type 1 gold. Inspection of the Ag profiles of alluvial gold (Figure 5A) suggests that around 60% of the particulate gold inventory is derived from a type of mineralization yet to be identified in either outcrop or float.

Outcome	Standard Exploration approaches: outcrop/float			Gold compositional studies		
	Proven	Inferred	Not possible	Proven	Inferred	Not possible
Characterise Mineralogy of ore	●				●	
Establish overall deposit paragenesis	●					●
Establish paragenesis of mineralization coeval with gold	○ [a]			●		
Identify genetic link between Au and other minerals	○	●		●		
Identify the extent of the vein array	●				●	
Identify the best drill target		●				●
Identify evidence for Au associations not observed in surface or in core			●	●		

Figure 11. Evaluation of the relative contributions of standard prospecting techniques and gold compositional studies to characterization of the LTVA. Hollow circles indicate that only partial information may be forthcoming. [a]: Full information is available from outcrops, but not all important outcrops may be discovered.

Visual evidence of complex vein paragenesis, evident in outcrops and float, and established during petrographic studies, could be inferred from the interpretation of the various alloy microfabrics observed in gold particles. However, gold particle studies have indicated which alloy types are potentially economically important. Finally, the ability to use specific mineral associations as indicators for magmatic hydrothermal systems is a strength of gold composition studies [47] and entirely consistent with the outcomes of previous studies on regional metallogeny [28,29,34].

5.3. Generic Considerations Regarding Adoption of Gold Compositional Studies as Part of an Exploration Strategy

Different exploration areas present different challenges to the adoption of gold compositional studies, and the potential to integrate outcomes with those from other approaches may also be site-specific. For instance, in the present study, the opportunity to correlate the signature of particulate gold from Lead Trial with detailed characterization of vein material from petrographic studies increased confidence in predicting further undiscovered mineralization suggested by alluvial gold signatures.

Classical exploration can identify gold-mineral associations through mineralogical study of float/outcrop/core, but gaining a comprehensive understanding of Au-mineral associations at the deposit scale through petrography may be compromised by sample availability from the whole mineralizing system, constraints on the number of mineralized samples that may be inspected in thin sections, and gold particle abundance. The potential for gold compositional studies to provide a wider overview of the important gold-ore associations than is logistically feasible through classical thin section petrography has been noted previously in studies at economically important gold localities of Cononish (Scotland), Curraghinalt (N. Ireland) and Atlin (British Columbia, Canada) [48]. Knowledge of the inclusion suite informs the design of subsequent geochemical surveys through the choice of an element suite that has a proven genetic association with gold. This removes the reliance on inferring these associations via gold-element covariance in spatial geochemical data sets. In addition, the geochemical data sets may themselves be compromised by the influence of the nugget effect on reported gold values and the resulting apparent gold-element associations.

The relative timescales and costs of gold compositional studies and standard exploration approaches vary enormously according to individual projects and preclude a generic quantitative approach to general comparative cost/benefit analysis. In the example reported here, two summer seasons of fieldwork by a small team of geologists culminated in a scout drilling program. In contrast, the collection of gold particles was completed by one field operative in under two weeks. Following two days of sample preparation, analysis by SEM and EPMA of these relatively large sample sets required 6–7 days. There may be challenges to undertaking gold compositional programs [25], not least the acquisition of the alluvial gold using specialized sampling approaches that sometimes require experienced operators. Standard stream sampling programs are superficially similar to gold collection activities, but they rarely recover sufficient gold particles to underpin gold compositional studies. During the current study, it proved very challenging to obtain gold particles from some points in Ardtalnaig Burn, both owing to restricted access because of the physical nature of the valley, and the scarcity of fluvial facies in which gold accumulates in sections of very steep gradient. Consequently, the amount of field time required to collect gold was longer than originally anticipated.

The particle size of gold liberated from the source provides a clear limit to the applicability of gold compositional studies, which are normally dependent on gold recovery by panning or hand sluicing. The recovery of gold by simple gravity concentration methods decreases markedly at sizes below 100 µm, and recovery of particles less than 60 µm is generally impractical [25]. Efficient workflow can also be compromised by the low incidence of inclusions in alluvial sample populations (e.g., 10%, Table 1). Low inclusion abundance may be either a consequence of the source mineralization or a result of obliteration resulting from fluvially induced alloy deformation [49,50]. Alluvial gold particles distal from the source may be difficult to characterize in the absence of an inclusion signature, but the degree of fluvial transport is unknown when commencing work in a new area. To some extent, this may be mitigated by speculating on the degree of fluvial transport through observation of the gold particle morphology [51], and decisions on sampling localities may be taken during the sampling program. Low inclusion incidence is impossible to predict when initiating a study, and exploration campaigns may not always have the capacity for repeat sampling. In addition, delineating the area of influx of gold into a fluvial system by sediment sampling can be both very time-consuming and ultimately inconclusive, as it is heavily influenced by both the nature of the fluvial setting at specific localities and the experience of the field operatives. Nevertheless, the speed at which the technique can yield results, and the potential to specify Au-mineral genetic associations and deposit type, can greatly inform initial approaches to more expensive follow-up procedures, whilst clearly guiding geochemical studies to the most important element pathfinders. The outcomes of the present work have highlighted mutual benefits to both methodologies that have been postulated in previous studies where commercial exploration preceded gold characterization, for example, in confirming the type of source mineralization of substantial placer gold in areas of the N. American Cordillera [37]. At Lead Trial, future exploration is alert to the presence of a local type of mineralization yet to be identified in either float or outcrop.

6. Conclusions

Integration of field prospecting, lithogeochemistry, soil geochemistry, and a ground-based magnetic survey undertaken in the LTVA provided robust evidence for the presence and extent of multiple auriferous veins of broadly similar nature. The most prospective area within the vein array generated a suitable drill target. Complex vein textures have been identified, and insights into complex vein paragenesis have been generated through classical petrographic studies.

Outcomes from gold compositional work overlap substantially with those derived from standard exploration approaches, i.e., the ability to broadly delineate the gold-bearing area, identify the most important gold-mineral associations, and provide evidence for both complex vein paragenesis and the geographical extent of important transient hydrothermal regimes. Notable disadvantages in relation to classical approaches are that complete characterization of all stages of mineralogy and paragenesis is not possible, although excellent data are generated for stages of mineralization coeval with gold. Gold compositional studies alone cannot generate drill targets, but they can provide proof of specific gold-mineral associations that may not be evident until standard exploration is advanced and mineralogical variations within the entire orefield are eventually established.

In most cases, compositional characteristics of gold particles within sample populations provide the means for mineralogical characterization, and in many alluvial gold districts, the approach can provide insights into the nature of source mineralization in the absence of any other geological context. This can be achieved at a cost far below standard scoping field studies, and in a relatively short time frame. Whilst adoption of the technique has found increasing use in academic studies in recent years, we believe it remains underutilized in industry, and where applied appropriately, it could constitute a potentially valuable tool in the early stages of exploration.

Author Contributions: Conceptualization, R.C., T.T. and A.L., methodology, R.C., T.T., A.L., K.D., G.D., S.W., L.S. and K.A., formal analysis, R.C. and R.W.; investigation, R.C., T.T., A.L., K.D., G.D., S.W., L.S. and K.A., data curation, R.C. and A.L.; writing—original draft preparation, R.C.; writing—review and editing, R.C., T.T., A.L., K.D., G.D., S.W., L.S. and K.A.; visualization, R.C. and T.T.; supervision, R.C. and T.T. All authors have read and agreed to the published version of the manuscript.

Funding: S.W (Grant No. 2445151) and L.S. (Grant No 2114866) were in receipt of NERC studentships.

Data Availability Statement: Data describing gold compositions are the property of the University of Leeds. Please contact Rob Chapman for further information. Data describing outcomes of exploration work are the property of Green Glen Minerals Limited. Please contact Aiden Lavelle for further information.

Acknowledgments: We are indebted to the Ardtalnaig and Milton Estates for providing access to the field areas.

Conflicts of Interest: The coauthors Aiden Lavelle and Kieran Armstrong are employed by the companies Green Glen Minerals Limited and Northern Star Resources Limited. Lucia Savastano is employed by the company Tescan. The remaining authors declare that the research was conducted in the absence of any commercial or financial relationships that could be construed as a potential conflict of interest.

References

1. McClenaghan, M.B.; Cabri, L.J. Review of gold and platinum group element (PGE) indicator minerals methods for surficial sediment sampling. *Geochem. Explor. Environ. Anal.* **2011**, *11*, 251–263. [CrossRef]
2. Chapman, R.J.; Torvela, T.M.; Savastano, L. Insights into regional metallogeny from detailed compositional studies of alluvial gold: An example from the Loch Tay area, Central Scotland. *Minerals* **2023**, *13*, 140. [CrossRef]
3. Chapman, R.J.; Mortensen, J.K. Characterization of gold mineralization in the northern Cariboo gold district, British Columbia, Canada, through integration of compositional studies of lode and detrital gold with historical placer production: A template for evaluation of orogenic gold districts. *Econ. Geol.* **2016**, *111*, 1321–1345. [CrossRef]
4. Chapman, R.J.; Moles, N.R.; Bluemel, B.; Walshaw, R.D. Detrital gold as an indicator mineral. In *Recent Advances in Understanding Gold Deposits: From Orogeny to Alluvium*; Torvela, T.M., Chapman, R.J., Lambert-Smith, J., Eds.; Geological Society, London, Special Publications; Geological Society of London: London, UK, 2022; Volume 516, pp. 313–336.

5. Savva, N.E.; Kravtsova, R.G.; Anisimova, G.S.; Palyanova, G.A. Typomorphism of native gold (geological-industrial types of gold deposits in the North-East of Russia). *Minerals* **2022**, *12*, 561.
6. Nikiforova, Z. Mineralogical method as an effective way to predict gold ore types of deposits in platform areas (East of the Siberian Platform). *Minerals* **2024**, *14*, 631. [CrossRef]
7. Fominykh, P.A.; Nevolko, P.A.; Svetlitskaya, T.V.; Kolpakov, V.V. Native gold from the Kamenka-Barabanovsky and Kharuzovka alluvial placers (Northwest Salair Ridge, Western Siberia, Russia): Typomorphic features and possible bedrock sources. *Ore Geol. Rev.* **2020**, *126*, 103781. [CrossRef]
8. Palyanova, G.A.; Proskurnin, V.F.; Silyanov, S.A.; Gavrish, A.V.; Belyaeva, T.V.; Borisenkov, K.V. Typomorphic features of placer gold from Bolshevik island of the Severnaya Zemlya Archipelago (Russia). *Geosci. Front.* **2025**, *16*, 102124. [CrossRef]
9. Nevolko, P.A.; Kolpakov, V.V.; Nesterenko, G.G.; Fominykh, P.A. Alluvial placer gold of the Egor'evsk District (Northern-Western Salair): Composition characteristics, types and mineral microinclusions. *Russ. Geol. Geophys.* **2019**, *60*, 67–85. [CrossRef]
10. Becerra, P.; Sanchez-Alfaro, P.; Piquer, J.; Plissart, G.; Garroz, B.; Kunstmann, D. Gold provenance in placers from Pureo area, Southern Chile Coastal Cordillera, and their relationship with Paleozoic metamorphic rocks. *Minerals* **2022**, *12*, 1147. [CrossRef]
11. Ngang, T.C.; Suh, C.E.; Wagner, T.; Bafon, T.G.; Fusswinkel, T.; Vishiti, A. Epithermal Ag–Au mineralization at Galim-Legalgorou, Cameroon Volcanic Line: Insights from alteration mineralogy and mineral chemistry of electrum and sphalerite. *Int. J. Earth Sci.* **2024**, *5*, 1285–1301. [CrossRef]
12. Omang, B.O. Microchemical characterization and stream sediment composition of alluvial gold particles from the Rafin Gora drainage system, Kushaka schist belt, North Western Nigeria. *Comm. Phys. Sci.* **2023**, *3*, 230–255.
13. Alam, M.; Li, S.R.; Santosh, M.; Yuan, M.W. Morphology and chemistry of placer gold in the Bagrote and Dainter streams, northern Pakistan: Impli cations for provenance and exploration. *Geol. J.* **2018**, *54*, 1672–1687. [CrossRef]
14. OberthÜr, T.; Melcher, F.; Weiser, T.W. Detrital platinum-group minerals and gold in placers of southeastern Samar Island, Philippines. *Can. Mineral.* **2017**, *55*, 45–62. [CrossRef]
15. Kolpakov, V.V.; Nevolko, P.A.; Fominykh, P.A. Mineralogy and primary sources of gold in the Davenda-Klyuchevskiy ore-placer cluster (Eastern Transbaikalia). *Geol. Ore Depos.* **2024**, *66*, 528–546. [CrossRef]
16. Svetlitskaya, T.V.; Nevolko, P.A.; Kolpakov, V.V.; Tolstykh, N.D. Native gold from the Inagli Pt Auplacer deposit (the Aldan Shield, Russia): Geochemical characteristics and implications for possible bed rock sources. *Miner. Depos.* **2018**, *53*, 323–338. [CrossRef]
17. Omang, B.O.; Suh, C.E.; Lehmann, B.; Vishiti, A.; Chombong, N.N.; Fon, A.N.; Egbe, J.A.; Shemang, E.M. Microchemical Signature of Alluvial Gold From Two Contrasting Terrains in Cameroon. *J. Afr. Earth Sci.* **2015**, *112*, 1–14. [CrossRef]
18. Saarnisto, M.; Tamminen, E.; Vaasjoki, M. Gold in bedrock and glacial deposits in the Ivalojoki area, Finnish Lapland. *J. Geochem. Explor.* **1991**, *39*, 303–322. [CrossRef]
19. dos Santos Alves, K.; Sánchez, S.B.; Barreiro, J.G.; Palomares, R.M.; Prieto, J.M. Morphological and compositional analysis of alluvial gold: The Fresnedoso gold placer (Spain). *Ore Geol. Rev.* **2020**, *121*, 103489. [CrossRef]
20. Gerasimov, B. The Use of typomorphic features of placer gold of the Anabar region for determining its sources. *Minerals* **2023**, *13*, 480. [CrossRef]
21. Lalomov, A.V.; Naumov, V.A.; Grigorieva, A.V.; Magazina, L.O. Evolution of the Vagran gold-bearing placer cluster (Northern Urals) and prospects for revealing bedrock mineralization. *Geol. Ore Depos.* **2020**, *5*, 407–418. [CrossRef]
22. Chapman, R.J.; Mortensen, J.K.; Crawford, E.C.; Lebarge, W. Microchemical studies of placer and lode gold in the Klondike District, Yukon, Canada: 1. Evidence for a small, gold-rich, orogenic hydrothermal system in the Bonanza and Eldorado Creek area. *Econ. Geol.* **2010**, *105*, 1369–1392. [CrossRef]
23. Nikiforova, Z. Internal Structures of Placer Gold as an Indicator of Endogenous and Exogenous Processes. *Minerals* **2023**, *13*, 68.
24. Palyanova, G.A. Editorial for the Special Issue "Native Gold as a Specific Indicator Mineral for Gold Deposits". *Minerals* **2023**, *13*, 1323. [CrossRef]
25. Moles, N.R.; Chapman, R.J. Integration of detrital gold microchemistry, heavy mineral distribution, and sediment geochemistry to clarify regional metallogeny in glaciated terrains: Application in the Caledonides of southeast Ireland. *Econ. Geol.* **2019**, *114*, 207–232. [CrossRef]
26. Chapman, R.J.; Torvela, T.M.; Spence-Jones, C.P.; Walshaw, R.D.; McLeod, G.W. Targeting High-Grade Mineralization via a Synthesis of Compositional Profiles of Alluvial Gold with Structural and Paragenetic Models. *Minerals* **2024**, *14*, 1236. [CrossRef]
27. Wilson, G.V.; Flett, J.S. Special Reports on the Mineral Resources of Great Britain. In *The Lead, Zinc, Copper and Nickel Ores of Scotland*; HMSO: London, UK, 1921; Volume 17.
28. Ixer, R.A.; Pattrick, R.A.; Stanley, C.J. Geology, mineralogy and genesis of gold mineralization at Calliachar-Urlar Burn, Scotland. *Trans. IMM Sect. B Appl. Earth Sci.* **1997**, *106*, 99–108.
29. Corkhill, C.; Ixer, R.A.; Mason, J.S.; Irving, D.; Pattrick, R.A. Polymetallic auriferous vein mineralization near Loch Tay, Perthshire, Scotland. *Scott. J. Geol.* **2010**, *46*, 23–30. [CrossRef] [PubMed]
30. Available online: https://www.scottishfinancialnews.com/articles/scotlands-only-gold-mine-restarts-as-prices-hit-record-highs (accessed on 20 April 2026).

31. Webb, S.; Torvela, T.; Chapman, R.; Savastano, L. *Textural Mapping and Building a Paragenetic Interpretation of Hydrothermal Veins*; Geological Society, London, Special Publications; Geological Society of London: London, UK, 2024; Volume 541, pp. 273–297. [CrossRef]
32. Pattrick, R. Sulphide mineralogy of the Tomnadashan copper deposit and the Corrie Buie lead veins, south Loch Tayside, Scotland. *Mineral. Mag.* **1984**, *48*, 85–91. [CrossRef]
33. Webb, S.; Torvela, T.; Chapman, R.; Selby, D.; Gooday, R. A reinterpretation of the mineralization processes involved in the formation of the Tomnadashan sulfide deposit, Loch Tay, Scotland, UK. *Scott. J. Geol.* **2024**, *60*, sjg2023-023. [CrossRef]
34. Webb, S.; Torvela, T.; Chapman, R.; Savastano, L.; Jamieson, R.; Boyce, A.; Tait, A.; Hollis, S.; Pashley, V. Constraining the fluid sources of gold-bearing veins in orogenic belts using sulfur and lead isotopes: A case study from Loch Tay, Scotland (UK). *Ore Geol. Rev.* **2025**, *181*, 106619. [CrossRef]
35. Thost, G.A. On the rocks, ores, and other minerals on the property of the Marquess of Breadalbane in the Highlands of Scotland. *Q. J. Geol. Soc.* **1860**, *16*, 421–428. [CrossRef]
36. Mason, J. (Erris Gold Resources Ltd, Perthshire, Scotland). Personal communication, 1980.
37. Chapman, R.J.; Mortensen, J.K.; Allan, M.M.; Walshaw, R.D.; Bond, J.; MacWilliam, K. A New Approach to Characterizing Deposit Type Using Mineral Inclusion Assemblages in Gold Particles. *Econ. Geol.* **2022**, *117*, 361–381. [CrossRef]
38. Lyell, C.M.; Stuart, F.M.; Shaw, J.I.; Boyce, A.J.; Cloutier, J. The role of mantle melting and associated granitoid magmatism in the genesis of orogenic gold in the Laurentian Caledonides. *Geology* **2026**, *54*, 184–188.
39. Savastano, L. Metallogeny of the Loch Tay Area (Central Scotland) from Gold Compositional Variations, Vein Parageneses and Structural Constraints. Ph.D. Thesis, University of Leeds, Leeds, UK, 2026.
40. Webb, S. Understanding metallogeny around Loch Tay, Scotland: Insights from Isotope Geochemistry and Petrographic Studies. Ph.D. Thesis, University of Leeds, Leeds, UK, 2024. Available online: https://etheses.whiterose.ac.uk/35121/.
41. Armstrong, K. Characterization of Gold Mineralization in the Lead Trial Prospect. Master's Thesis, University of Exeter, Exeter, UK, 2021.
42. Chapman, R.J.; Banks, D.A.; Styles, M.T.; Walshaw, R.D.; Piazolo, S.; Morgan, D.J.; Grimshaw, M.R.; Spence-Jones, C.P.; Matthews, T.J.; Borovinskaya, O. Chemical and Physical Heterogeneity Within Native Gold: Implications for the Design of Gold Particle Studies. *Miner. Depos.* **2021**, *56*, 1563–1588. [CrossRef]
43. Leake, R.C.; Chapman, R.J.; Bland, D.J.; Condliffe, E.; Styles, M.T. Microchemical Characterization of Alluvial Gold from Scotland. *Trans. Inst. Min. Metall. (Sect. B Appl. Earth Sci.)* **1997**, *106*, B85–B98.
44. Warr, L.N. IMA–CNMNC approved mineral symbols. *Mineral. Mag.* **2021**, *3*, 291–320. [CrossRef]
45. Gammons, C.H.; Williams-Jones, A.E. Hydrothermal Geochemistry of Electrum; Thermodynamic Constraints. *Econ. Geol.* **1995**, *90*, 420–432. [CrossRef]
46. Chudnenko, K.V.; Palyanova, G.A. Thermodynamic modelling of native formation of Au–Ag–Cu Hg solid solutions. *Appl. Geochem.* **2016**, *66*, 88–100. [CrossRef]
47. Chapman, R.J.; Mortensen, J.K.; Murphy, R. Compositional Signatures of Gold from Different Deposit Types in British Columbia, Canada. *Minerals* **2023**, *13*, 1072. [CrossRef]
48. Spence-Jones, C.P. Geochemical Signatures of Native Gold Alloys as a Tool for Understanding Auriferous Ore Deposits. Ph.D. Thesis, University of Leeds, Leeds, UK, 2021.
49. Loen, J.S. Use of placer gold characteristics to locate bedrock gold mineralization. *Explor. Min. Geol.* **1995**, *4*, 335–339.
50. Melchiorre, E.B.; Henderson, J. Topographic gradients and lode gold sourcing recorded by placer gold morphology, geochemistry, and mineral inclusions in the east fork San Gabriel River, California, USA. *Ore Geol. Rev.* **2019**, *109*, 348–357. [CrossRef]
51. Masson, F.X.; Beaudoin, G.; Laurendeau, D. *Multi-method 2D and 3D reconstruction of gold grain morphology in alluvial deposits: A review and application to the Rivière du Moulin (Québec, Canada) In Recent Advances in Understanding Gold Deposits: From Orogeny to Alluvium*; Torvela, T.M., Chapman, R.J., Lambert-Smith, J., Eds.; Geological Society, London, Special Publications; Geological Society of London: London, UK, 2022; Volume 516, pp. 337–352.